



Perfluorooctane Sulfonate Exposure Induces Cardiovascular Dysfunction in Female Rats: Role of Ovaries

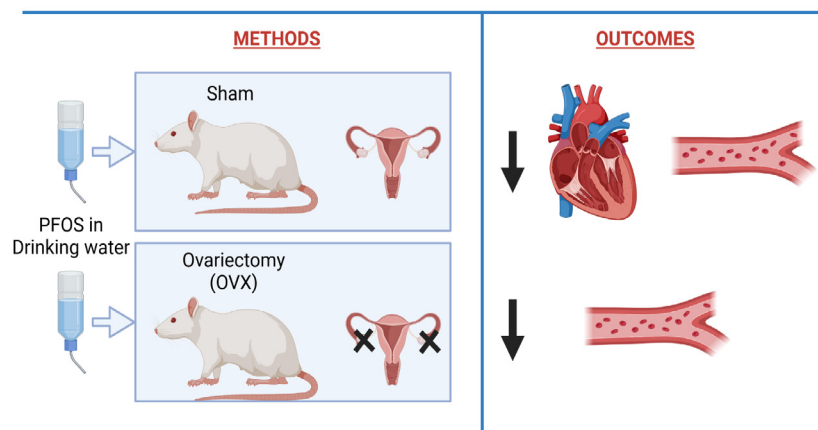
Karina Porfirio¹, Pankaj Yadav¹, Sri Vidya Dangudubiyam¹, Alissa Hofmann¹, Jay S. Mishra¹, Sathish Kumar^{1,2*}

Abstract

Per-and polyfluoroalkyl substances (PFAS) are pervasive environmental pollutants frequently detected in drinking water worldwide. Reports linking PFAS exposure to cardiovascular disease have increased significantly in recent years. Furthermore, women appear to be more susceptible to the adverse effects of PFAS. However, the potential role of ovaries in the increased vulnerability of females to PFAS-related health effects remains unknown. In this study, we investigated the impact of perfluorooctane sulfonate (PFOS), a prominent PFAS, on the cardiovascular function in female rats with intact ovaries and ovariectomized (OVX) females. Bilateral OVX or sham surgeries were performed in 8-week-old female SD rats. Following recovery from surgeries, the rats were given drinking water containing 50 µg/mL of PFOS for 3 weeks. Control groups received PFOS-free water. PFOS exposure significantly reduced body weight but increased blood pressure similarly in both intact and OVX rats. Echocardiography analysis revealed that PFOS exposure decreased cardiac output, end-systolic volume, and end diastolic volume in intact but not OVX rats. Vascular function studies demonstrated that PFOS equally reduced endothelium-dependent and -independent relaxation responses in intact and OVX rats. The endothelium-independent contractile responses were more pronounced in both intact and OVX rats. eNOS protein levels were similarly decreased in both intact and OVX rats. In conclusion, PFOS affects cardiac function through hormone-dependent mechanisms, while vascular function is impaired independent of ovarian status, indicating an intricate interplay between PFOS exposure, ovarian status, and cardiovascular function.

Graphical Abstract

PFOS impairs cardiac function through ovary-dependent mechanisms, while vascular function is impaired independent of ovaries.



Affiliation:

¹Department of Comparative Biosciences, School of Veterinary Medicine, University of Wisconsin, Madison, Wisconsin, United States of America

²Department of Obstetrics and Gynecology, School of Medicine and Public Health, University of Wisconsin, Madison, Wisconsin, United States of America

*Corresponding authors:

Sathish Kumar, Department of Comparative Biosciences, School of Veterinary Medicine, University of Wisconsin, Madison, Wisconsin, United States of America.

Citation: Karina Porfirio, Pankaj Yadav, Sri Vidya Dangudubiyam, Alissa Hofmann, Jay S. Mishra, Sathish Kumar. Perfluorooctane Sulfonate Exposure Induces Cardiovascular Dysfunction in Female Rats: Role of Ovaries. *Cardiology and Cardiovascular Medicine*. 8 (2024): 275-284.

Received: June 11, 2024

Accepted: June 17, 2024

Published: June 26, 2024

Keywords: Perfluorooctane sulfonate (PFOS); Cardiovascular Dysfunction; Vascular Reactivity; Endothelial Dysfunction; Nitric Oxide Synthase; Ovariectomy; Environmental Pollutants

Introduction

Cardiovascular diseases are the primary cause of death and illness in the US, with hypertension being the most prevalent form, affecting nearly one-third of adults [1]. While current therapies focus on lowering blood pressure, identifying and targeting the underlying causes is crucial for effective treatment. Although genetic factors play a role [2], environmental exposures, such as per- and poly-fluoroalkyl substances (PFAS), are increasingly recognized as significant contributors to the rising prevalence of hypertension [3-5]. PFAS comprise a vast and diverse class of approximately more than 5,000 synthetic organofluorine compounds. Due to their water-, heat-, stain-, and grease-repellent properties, PFAS are extensively utilized in a wide array of industrial and consumer products, including stain-resistant textiles, food packaging, surfactants, firefighting foams, insecticides, and coatings. Among the numerous PFAS compounds, perfluorooctane sulfonate (PFOS) is a legacy compound and the most extensively produced and studied representative of this class. PFOS exhibits high environmental persistence due to its non biodegradable nature and chemical stability, leading to its designation as a "forever chemical"[6]. Drinking water serves as the primary exposure route for in humans. Alarmingly, many public water systems in the United States exhibit PFOS concentrations surpassing the Environmental Protection Agency's (EPA) health advisory limit of 70 ng/L [7, 8]. Reports indicate that 194 public water systems, serving approximately 16.5 million people, exceed this threshold, with some systems reaching levels as high as 1800 ng/L [9]. Notably, even local water sources in Madison, Wisconsin, and surrounding areas, including lakes and creeks, exhibit elevated PFOS levels [10, 11]. Furthermore, PFOS contamination has been detected in packaged and bottled water [12]. Following exposure, PFOS undergoes bioaccumulation within the human body, with an estimated half-life of up to 5.4 years [13, 14]. Federal and state agencies, including the National Institute of Environmental Health Sciences (NIEHS) and EPA, recognize PFOS as a persistent biohazard posing significant long-term health risks [15-17]. Consequently, there is a need to investigate PFOS's biological effects to inform risk assessment and public policy development.

To date, five epidemiological studies have reported a positive correlation between elevated PFOS levels and hypertension in humans [3, 18-21]. Notably, these studies indicate a significant sex-dependent effect, with PFOS exposure exhibiting a stronger association with hypertension in women compared to men. For example, a positive association was observed between PFOS and hypertension incidence

among 1058 multi-racial/ethnic middle-aged women [22]. Similarly, stronger positive correlations between systolic blood pressure and PFOS levels were noted in women than in men [23, 24]. While an association between PFOS exposure and hypertension has been established, a causal relationship remains to be elucidated. Controlled animal studies are necessary to definitively determine if PFOS directly induces hypertension. Previous studies suggest that the presence of intact ovaries might contribute to the heightened susceptibility of females to PFOS-related health effects [25, 26]. Thus, we further sought to investigate the influence of ovariectomy (OVX) on the cardiovascular function of female rats exposed to PFOS. Given the well-established impact of OVX on cardiovascular function, our primary objective was to focus on how PFOS exposure affects cardiovascular function in ovary-intact vs. OVX rats.

Materials and Methods

Animals

All animal experiments were conducted in accordance with the National Institutes of Health guidelines and approved by the Institutional Animal Care and Use Committee at the University of Wisconsin-Madison. Twenty four eight-week-old female Sprague-Dawley rats (Envigo Laboratories) were randomly assigned to four groups (n=6 per group): 1) intact ovaries control, 2) intact ovaries PFOS-exposed, 3) OVX control, and 4) OVX PFOS-exposed. PFOS-exposed groups received drinking water containing 50 µg/mL PFOS for three weeks, while control groups received PFOS-free water (vehicle). The PFOS dosage was selected based on prior research and aligns with concentrations observed in high-exposure areas [27, 28]. Rats were maintained in a controlled environment with a 12:12-hour light-dark cycle and provided standard breeder chow ad libitum. Body weight, food/water intake, and blood pressure were monitored weekly. Echocardiography was performed after three weeks of exposure, followed by euthanasia and tissue collection. Plasma, mesenteric arteries (for vascular function and molecular analyses), and left ventricles (for histopathology) were harvested for further analysis.

Blood Pressure Measurements

For blood pressure assessment, rats were gently restrained in nose cone devices and fitted with non-invasive tail cuffs (Kent Scientific, Torrington, CT). A two-day acclimation period was provided, wherein rats were placed on a 30°C warming chamber for 10 minutes to promote tail vasodilation prior to blood pressure measurement. Occlusion and volume pressure-recording cuffs were secured at the tail base and programmed for automated inflation/deflation cycles within a 90-second timeframe. Initial measurements from the first five cycles were discarded as acclimation data. Subsequent cycles were averaged to determine the mean blood pressure for each rat. Data was recorded and analyzed using Kent Scientific software.

Echocardiography

Rats were anesthetized with 2% isoflurane in oxygen and maintained on a heated platform throughout the procedure. Cardiac function was assessed using transthoracic M-mode, B-mode, and pulsed Doppler echocardiography (Vevo 3100; VisualSonics, Toronto, ON, Canada) equipped with an MS250 probe (13-24 MHz frequency, 30- μ m resolution, 240 frames per second). This methodology aligns with previous studies and enables accurate assessment of various cardiac parameters. Aortic diameter was measured distal to the aortic valve, and heart rate was determined from pulsed-wave Doppler tracings of the left ventricular outflow tract. End-diastolic and end-systolic left ventricular (LV) diameter, along with LV anterior wall (LVAW) and posterior wall (LVPW) thickness, were measured from M-mode images acquired in a parasternal long-axis view using the leading-edge-to-leading-edge convention. For each parameter, measurements were obtained for a minimum of three consecutive cycles and averaged. All echocardiographic images and measurements were performed by a single individual to ensure consistency. Cardiac parameters were calculated using Vevo 3100 software. Fractional shortening was determined as [(LV diameter diastole – LV diameter systole)/LV diameter diastole] x 100. Ejection fraction was calculated as [(7.0/(2.4 + LV diameter diastole) (LV diameter diastole)³ – (7.0/(2.4 + LV diameter systole)(LV diameter systole)³)/(7.0/(2.4 + LV diameter diastole) (LV diameter diastole)³ × 100)]. LV mass was calculated as [1.05 × ((posterior wall diastole + anterior wall diastole + LV diameter diastole)³ – (LV diameter diastole)³)]

Ex-vivo Vascular Reactivity Studies

The mesenteric arterial branches originating from the internal iliac artery were excised and cleared free of any adherent connective tissue. Segments of the artery, measuring 2 mm in length, were mounted on a wire myograph (Danish Myo Technology, Aarhus, Denmark) for isometric tension recording. The segments were immersed in Krebs physiological solution (KPS) comprising NaCl (118 mM), KCl (4.7 mM), CaCl₂ (2.5 mM), MgSO₄ (1.2 mM), KH₂PO₄ (1.2 mM), NaHCO₃ (25 mM), and glucose (11.1 mM). Following a one-hour equilibration period at resting tension in KPS, the arterial rings were normalized using Myodata software (Danish Myotechnology). Endothelial integrity was maintained for designated rings, while in others, the endothelium was denuded using tungsten wire. Successful endothelial denudation was confirmed by the absence of acetylcholine (ACh)-induced relaxation in phenylephrine (PE)-precontracted rings.

Contractile Responses

Arterial segments were initially exposed to 80 mM potassium chloride (KCl) to induce depolarization and elicit consistent contractile responses. Then, cumulative

concentration-response curves to PE (10⁻⁹ to 3 x 10⁻⁵ M) and U46619 (thromboxane A2 mimetic, 10⁻¹¹ to 10⁻⁷ M) were generated to assess vascular smooth muscle contractility.

Relaxation Responses

To evaluate endothelium-dependent relaxation, ACh induced relaxation (10⁻⁹ to 10⁻⁵ M) was measured in PE-precontracted arteries with intact endothelium. For endothelium-independent relaxation, sodium nitroprusside (SNP)-induced relaxation (10⁻⁹ to 10⁻⁵ M) was assessed in PE-precontracted arteries following endothelial denudation. In both cases, the PE concentration eliciting 80% of the maximal contractile response was utilized for precontraction.

RNA Isolation and Quantitative Real-Time Polymerase Chain Reaction

Total RNA was isolated from mesenteric arteries using an RNeasy mini kit (QIAGEN, Valencia, CA). RNA concentration and integrity were assessed using a Nanodrop spectrophotometer (ThermoFisher Scientific, Newark, DE). One microgram of total RNA was reverse transcribed into cDNA using an iScript cDNA synthesis kit (Bio Rad, Hercules, CA). Subsequently, cDNA equivalent to 3 ng of RNA was amplified via quantitative real-time reverse transcription polymerase chain reaction (qRT-PCR) on a CFX96 real-time thermal cycler (Bio-Rad), employing TaqMan Gene Expression Assays (Invitrogen; Thermo Scientific, Grand Island, NY) with FAM as the fluorophore. PCR conditions consisted of an initial cycle of 2 minutes at 50°C and 10 minutes at 95°C, followed by 50 cycles of 15 seconds at 95°C and 1 minute at 60°C. All reactions were performed in duplicate with a 10 μ L reaction volume containing a final concentration of 250 nM TaqMan probe and 900 nM of each primer.

Western Blotting

Mesenteric arteries were homogenized in ice-cold radioimmunoprecipitation assay buffer (Cell Signaling Technology, Danvers, MA) and centrifuged (10 minutes, 4°C). Supernatant protein concentration was determined using the Pierce BCA protein assay kit (Thermo Scientific, Waltham, MA). Following sample preparation with NuPAGE sample buffer and reducing agent (Invitrogen; Thermo Scientific, Waltham, MA), 30 μ g of protein per sample were resolved via electrophoresis on 4-12% gradient NuPAGE Bis-Tris gels (Invitrogen) at 100 V for 2 hours. Proteins were then transferred to Immobilon-P membranes (Millipore Inc, Billerica, MA) using a mini-Blot Module (Invitrogen) at 20 V for 1 hour. After blocking with 5% skim milk, membranes were probed overnight with primary antibodies against eNOS (rabbit monoclonal, #32027, Cell Signaling Technologies, Danvers, MA) and GAPDH (rabbit monoclonal, #5174, 1:1000, Cell Signaling Technologies, Danvers, MA). Subsequent incubation with horseradish peroxidase-conjugated anti-rabbit secondary antibodies

(1 hour) allowed for protein detection using Pierce enhanced chemiluminescence kits (Thermo Scientific, Waltham, MA). Densitometric analysis was performed with ImageJ software, and results were normalized to GAPDH expression.

Histopathological analysis

Left ventricular sections were fixed and embedded in paraffin wax, subsequently sectioned into 5- μ m slices, and stained with Hematoxylin and Eosin (H&E). The extent of left ventricular wall thickness and any fibrotic regions were quantified using ImageJ software. Colorimetric thresholding was employed to delineate blue-stained areas within each tissue section, corresponding to collagen deposition and fibrosis.

Statistical Analysis

Statistical analyses were conducted using GraphPad Prism software (San Diego, CA). Data are presented as mean \pm standard error of the mean (SEM). Cumulative concentration-response curves were analyzed using a

four-parameter logistic model. Contractile responses to PE were expressed as a percentage of the maximum PE-induced contraction. Relaxant responses to ACh and SNP were expressed as a percentage of the PE-induced precontraction. ANOVA with Dunnett's post hoc was used for comparisons. Statistical significance was established at $p \leq 0.05$.

Results

Body Weights and Blood Pressure

Progressive changes in body weight gain and blood pressure are shown in Figure 1A and B. After 3 weeks, PFOS exposure significantly reduced body weight gain in both intact and OVX rats compared to their respective control groups (Figure 1C). However, PFOS exposure did not significantly affect food or water intake in either group (data not shown). Exposure to PFOS resulted in a significant elevation of blood pressure in both intact and OVX rats compared to their respective control groups (Figure 1D).

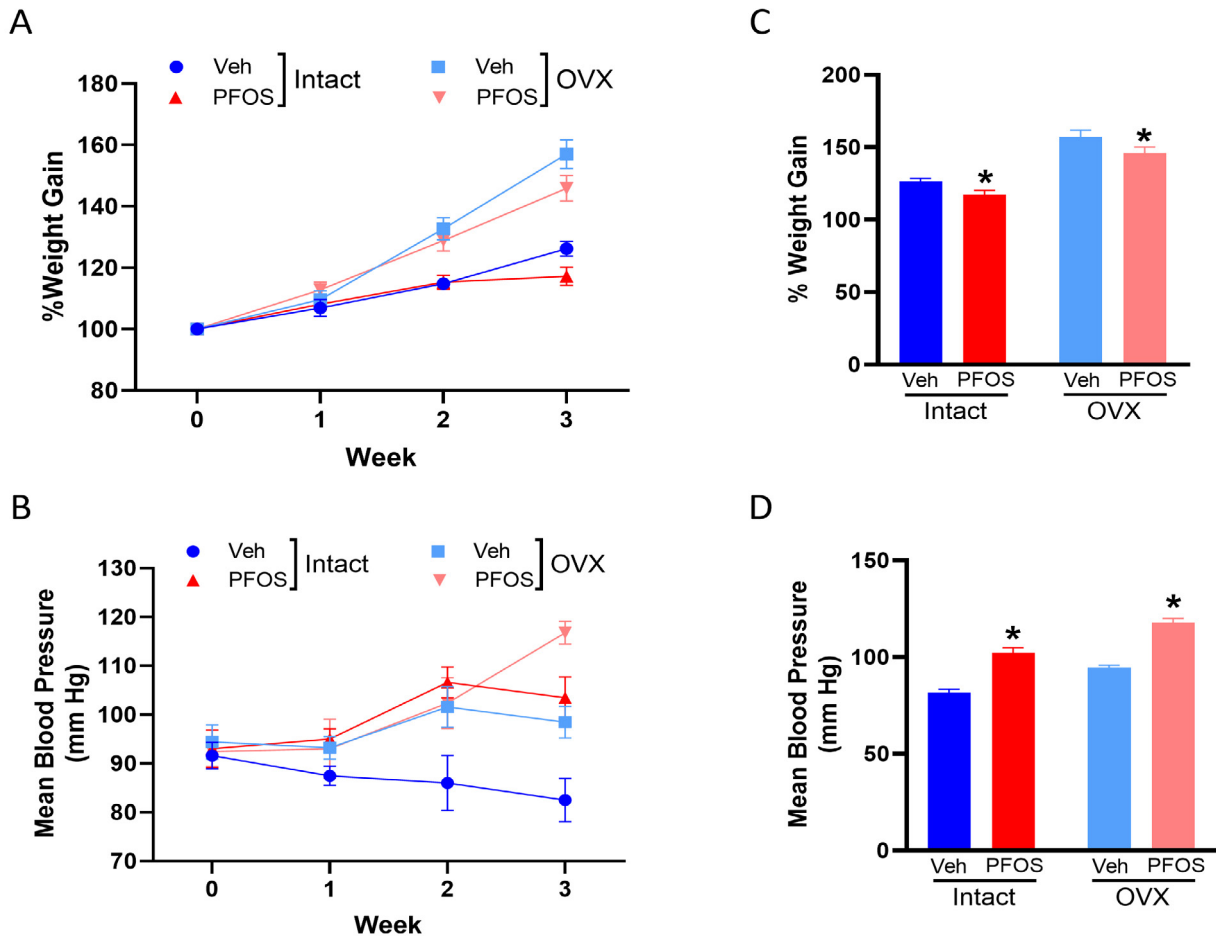


Figure 1: Effect of PFOS on body weight and blood pressure response. In the 8-week-old female SD rats, bilateral ovariectomy (OVX) or sham surgeries were performed. After recovery, rats were divided into four groups, i.e., intact ovaries control, PFOS-exposed, OVX control, and PFOS-exposed. Rats received drinking water containing 50 μ g/mL PFOS for three weeks, while control groups received PFOS-free water. (A) Percent body weight gain and (B) blood pressure changes each week. (C) Percent body weight gain and (D) Blood pressure at the end of 3 weeks. Data are means \pm SEM of 6 rats per group. * $p \leq 0.05$ compared to their respective vehicle control group.

Contractile Responses

PFOS exposure did not significantly alter KCl-induced (depolarization-induced) contractile responses in endothelium-denuded mesenteric arteries (Figure 2A). However, PFOS exposure potentiated contractile responses to both PE (α 1-adrenoreceptor agonist, Figure 2B) and U46619 (thromboxane A2 mimetic, Figure 2C) in endothelium-denuded mesenteric arteries, as evidenced by increased maximal responses in both intact and OVX rats compared to their respective controls (Figure 2B and C).

Relaxation Responses

PFOS exposure significantly attenuated endothelium-dependent relaxation responses to ACh in both intact and OVX rats compared to their respective control groups (Figure 3A). Conversely, PFOS exposure did not significantly alter endothelium-independent relaxation responses to SNP in either intact or OVX rats compared to controls (Figure 3B).

eNOS Expression

PFOS exposure significantly reduced the expression of eNOS mRNA and protein in the mesenteric arteries of both intact and OVX rats compared to their respective control groups (Figure 4).

Echocardiography and Histopathology

In intact female rats, PFOS exposure significantly reduced cardiac output, systolic volume, and diastolic volume (Figure 5). However, these effects were not observed in OVX rats (Figure 5). Furthermore, PFOS exposure did not significantly impact heart rate, stroke volume, ejection fraction, or fractional shortening in either intact or OVX rats (Figure 5).

Additionally, gross structural analysis of left ventricular wall thickness revealed no significant alterations in both intact and OVX rats following PFOS exposure (Figure 6).

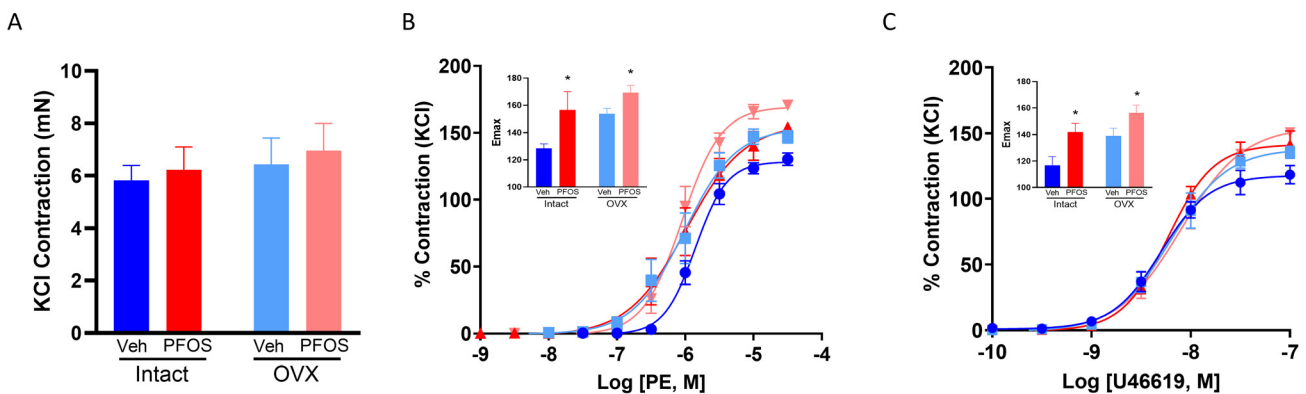


Figure 2: Effect of PFOS on endothelium-denuded mesenteric artery contractility in intact and OVX females. Mesenteric artery rings were obtained from vehicle (veh) or PFOS exposed intact and OVX females. Vascular contractile responses were taken to (A) KCl (80 mM), and to cumulative additions of (B) phenylephrine (PE) and (C) thromboxane analogue (U46619). * $p \leq 0.05$ compared to their respective vehicle control groups. Data are means \pm SEM of 6 rats per group.

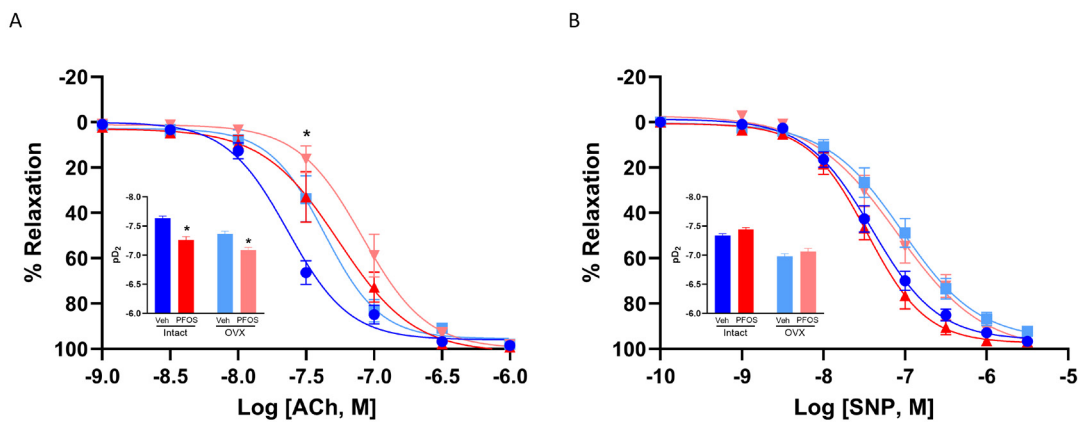


Figure 3: Effect of PFOS on mesenteric artery relaxation responses in intact and OVX females. Mesenteric artery rings were obtained from vehicle (veh), or PFOS exposed intact and OVX females. (A) Endothelium-dependent relaxation. Mesenteric arterial rings were precontracted with PE and examined for relaxation to ACh. (B) Endothelium-independent relaxation. Mesenteric arterial rings were precontracted with PE and examined for relaxation to cumulative additions of SNP. * $p \leq 0.05$ compared to their respective vehicle control groups. Data are means \pm SEM of 6 rats per group.

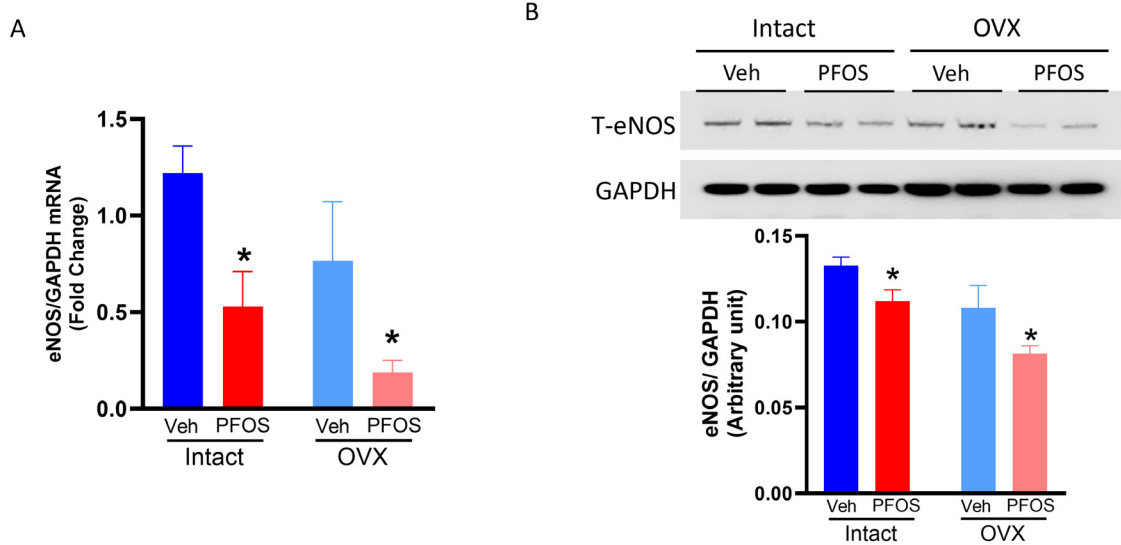


Figure 4: Effect of PFOS on mesenteric arterial eNOS mRNA and protein levels in intact and OVX females.

(A) eNOS mRNA expression was measured using real-time reverse transcriptase PCR and normalized relative to GAPDH levels. (B) eNOS protein was measured by Western blotting. Representative blots are shown at the top and densitometric values are shown at the bottom. * $p \leq 0.05$ compared to their respective vehicle control groups.

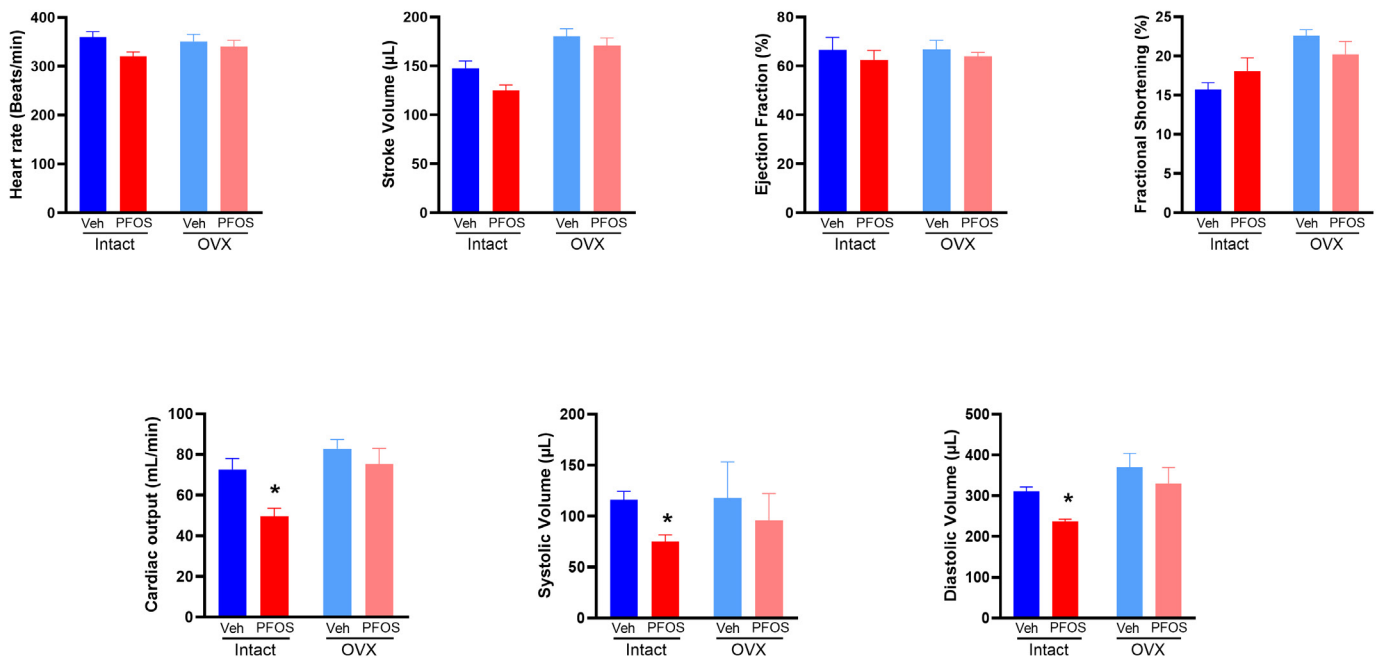


Figure 5: Effect of PFOS on echocardiography parameters in intact and OVX females. Heart rate, stroke volume, ejection fraction, fractional shortening, cardiac output, end-systolic volume, and end-diastolic volume parameters were evaluated from at least 3 adjacent cardiac cycles and expressed as mean values. Data are means \pm SEM of 6 rats per group. * $p \leq 0.05$ compared to their respective vehicle control groups.

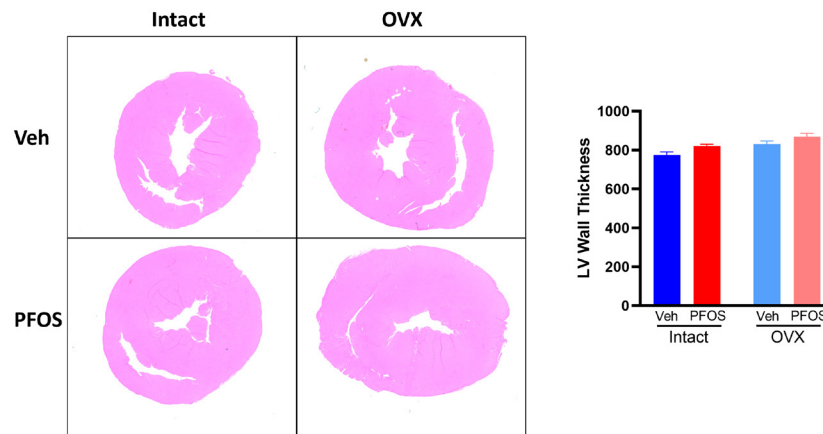


Figure 6: Effect of PFOS on left ventricular wall thickness in intact and OVX females. Left ventricular wall thickness were measured following hematoxylin and eosin staining and quantified using ImageJ software. Data are means \pm SEM of 6 rats per group.

Discussion

The objective of this study was to investigate whether PFOS exposure induces hypertension and impairs cardiovascular function in female rats with intact ovaries and OVX females. The main findings of the study are as follows: 1) PFOS exposure induced a reduction in body weight gain in both intact and OVX rats without affecting food or water intake. 2) PFOS exposure led to elevated blood pressure in both intact and OVX rats. 3) PFOS exposure enhanced vascular smooth muscle contractility in response to PE and U46619, independent of the endothelium in both intact and OVX rats. 4) PFOS exposure impaired endothelium-dependent relaxation (ACh-induced) while leaving endothelium-independent relaxation (SNP-induced) unaffected in both intact and OVX rats. 5) PFOS exposure decreased eNOS expression in mesenteric arteries of both intact and OVX rats. 6) PFOS exposure induced cardiac dysfunction (reduced cardiac output, systolic volume, and diastolic volume) in intact rats but not in OVX rats. Other cardiac parameters remained unaffected. These results indicate that PFOS exposure differentially affects cardiovascular function depending on the presence of ovaries. Specifically, PFOS-induced cardiac dysfunction appears to be modulated by ovaries, whereas vascular dysfunction occurs independent of ovaries.

Numerous cross-sectional and longitudinal observational studies have reported an increased incidence of cardiovascular disease and mortality associated with environmental pollutant exposure, with evidence suggesting a correlation with early vascular lesions [3]. In the current study, we observed a significant reduction in body weight gain in both intact and OVX female rats exposed to PFOS compared to their respective controls. This reduction was not attributable to differences in food or water intake, as both control and PFOS-exposed groups exhibited similar consumption patterns. The mechanisms underlying this PFOS-induced weight loss remain elusive and warrant further investigation. Future research should explore the potential effect of PFOS on

energy expenditure, metabolic pathways, and adipose tissue distribution to elucidate the precise mechanisms contributing to the observed weight loss phenotype.

Our study demonstrated that PFOS exposure induced an increase in blood pressure in female rats, aligning with previous human studies that reported stronger associations between PFAS exposure and blood pressure in women compared to men [23]. Furthermore, research by Bao et al. [24] regarding sex-specific effects also indicated heightened sensitivity to PFAS-induced blood pressure elevation in women. While it has been proposed that PFAS accumulation in female gonads may contribute to this increased susceptibility [25, 26], our findings of PFOS-induced hypertension in both intact and ovariectomized females suggest that these effects may be independent of gonadal influence. Further investigation is warranted to elucidate the precise mechanisms underlying the sex-specific and gonadal influence on PFOS-induced effects on blood pressure regulation.

To assess the impact of PFOS exposure on vascular function in female rats, we examined vascular contractile responses. Our study revealed a significant increase in both U46619- and PE-induced contractions in endothelium-denuded mesenteric arteries of ovary-intact PFOS-exposed rats, indicating heightened arterial sensitivity to contractile agonists. However, the lack of difference in KCl-induced depolarization-mediated contractions between PFOS and control groups suggests that the augmented agonist-induced contractions in PFOS-exposed rats are not attributable to alterations in vascular wall thickness or remodeling. The observed increase in agonist-mediated vascular contractions may reflect changes in the expression or function of their respective receptors. Notably, previous studies have demonstrated that PFOS exposure upregulates angiotensin type-1 receptor expression, leading to enhanced vasoconstriction in pregnant rat uterine arteries [29]. Further investigation is warranted to determine whether PFOS modulates other receptors or downstream signaling events

in non-pregnant conditions. Interestingly, the enhanced U46619- and PE-induced contractions were also observed in ovariectomized rats, suggesting that PFOS-induced exaggerated vascular smooth muscle contractility occurs independently of endothelial function and ovarian hormonal status.

This study demonstrates that PFOS exposure attenuates ACh-induced relaxation in mesenteric arteries of both intact and ovariectomized rats. Given the crucial role of NO as an endothelium-derived vasodilator [30], the observed inhibition of ACh-induced relaxation by PFOS could be attributed to either a decrease in NO synthesis and release from endothelial cells or a reduced sensitivity of vascular smooth muscle to NO. However, the lack of difference in SNP-induced relaxation of endothelium-denuded mesenteric arteries between PFOS-exposed and control groups indicates that PFOS does not affect vascular smooth muscle sensitivity to relaxation. This suggests that the attenuated ACh-induced relaxation in PFOS-exposed rats is likely due to impaired endothelial NO production. The precise mechanism underlying this impairment remains unclear, but it may involve alterations in eNOS expression or activity. Our findings of decreased eNOS mRNA and protein levels in the mesenteric arteries of PFOS-exposed rats support this hypothesis. Several upstream factors regulate eNOS expression, including vascular endothelial growth factor (VEGF). PFOS has been shown to downregulate VEGF signaling in endothelial cells [31], suggesting a potential VEGF-dependent mechanism for PFOS-induced eNOS suppression and subsequent endothelial dysfunction. Further investigation is required to elucidate this mechanism. The observation of similar vasodilatory responses and eNOS expression patterns in both ovary-intact and OVX rats exposed to PFOS indicates that PFOS-induced vascular effects occur independently of ovarian influence.

In this study, echocardiography was utilized to assess cardiac function, revealing that PFOS exposure significantly reduced cardiac output, systolic volume, and diastolic volume in non-pregnant female rats. This contrasts with previous findings in pregnant rats, where PFOS exposure increased stroke volume, ejection fraction, and fractional shortening [29]. This discrepancy may be attributed to the distinct physiological adaptations of the cardiovascular system during pregnancy, including elevated cardiac output and stroke volume to accommodate fetal demands [32]. Interestingly, the observed PFOS-induced reduction in cardiac output, systolic volume, and diastolic volume was exclusive to ovary-intact rats and not in OVX rats, suggesting a potential role for ovarian hormones in mediating these effects. Given that *in vitro* bioassays have demonstrated PFOS's weak estrogenic activity and its ability to activate estrogen receptor alpha (ER α) *in vivo* [33, 34], it is plausible that PFOS may interact with ovarian hormones or their receptors, exacerbating cardiac dysfunction in intact females but not in OVX females lacking these hormonal influences. Further research is warranted to elucidate the precise mechanisms

underlying this interaction and its potential implications for PFOS-induced cardiotoxicity in females.

Conclusion

In summary, this study revealed that PFOS exposure altered vascular function through ovary-independent mechanisms by increasing vascular resistance and increasing arterial pressure. This study also revealed that PFOS exposure impaired cardiac function through ovary-dependent mechanisms by decreasing cardiac output, systolic volume, and diastolic volume. These findings highlight the complex interplay between PFOS exposure, ovarian hormones, and cardiovascular health, with implications for sex-specific risk assessment and targeted interventions for PFOS-induced cardiovascular disease.

Author Contributions

K.P., P. Y., S.D., and J.M. participated in concept development and study design, performed experimental work, data analysis and drafted the manuscript; A. H. performed experimental work; S.K. conceived the conception and study design, obtained funding, provided important intellectual support, and edited the manuscript. All authors have seen and approved the final version.

Funding

Financial Support from the National Institute of Health (NIH) through grants R01ES033345 and T35OD011078 is greatly appreciated. The content is solely the authors' responsibility and does not necessarily represent the official views of NIH. The funding agency was not involved in the design, analysis, or interpretation of the data reported.

Data Availability

All data are incorporated into the article and available upon request.

Declarations Conflict of interest

Authors declare no conflict of interest.

References

1. High Blood Pressure. Centers for Disease Control and Prevention. (2023). <http://www.cdc.gov/bloodpressure/>.
2. Delles C, McBride MW, Graham D, et al. Genetics of hypertension: from experimental animals to humans. *Biochim Biophys Acta* 1802 (2010): 1299-1308.
3. Meneguzzi A, Fava C, Castelli M, et al., Exposure to Perfluoroalkyl Chemicals and Cardiovascular Disease: Experimental and Epidemiological Evidence. *Front Endocrinol (Lausanne)* 12 (2021): 706352.
4. Ou Y, Zeng X, Lin S, et al. Gestational exposure to perfluoroalkyl substances and congenital heart defects: A nested case-control pilot study. *Environ Int* 154 (2021): 106567.

5. Zhou R, Cheng W, Feng Y, et al. Combined effects of BPA and PFOS on fetal cardiac development: In vitro and in vivo experiments. *Environ Toxicol Pharmacol* 80 (2020): 103434.
6. Lindstrom AB, Strynar MJ, Libelo EL. Polyfluorinated compounds: past, present, and future. *Environ Sci Technol* 45 (2011): 7954-7961.
7. Anderko L, Pennea E, Chalupka S. Per- and Polyfluoroalkyl Substances: An Emerging Contaminant of Concern. *Annu Rev Nurs Res* 38 (2019): 159-182.
8. Silver, M, William P, Kevin M, Kyle B, et al. Prevalence and Source Tracing of PFAS in Shallow Groundwater Used for Drinking Water in Wisconsin, USA. *Environmental Science & Technology*. 45 (2023): 17415-17426.
9. Hu XC, Andrews DQ, Lindstrom AL. et al. Detection of Poly- and Perfluoroalkyl Substances (PFASs) in U.S. Drinking Water Linked to Industrial Sites, Military Fire Training Areas, and Wastewater Treatment Plants. *Environ Sci Technol Lett* 3 (2016): 344-350.
10. City of Madison. Perfluorinated Compounds. (2022). <https://www.cityofmadison.com/water/water-quality/perfluorinated-compounds>.
11. Mills S. Concerns Over PFAS Prompt New Fish Consumption Advisory In Madison. (2020). <https://www.wpr.org/concerns-over-pfas-prompt-new-fish-consumption-advisory-madison>.
12. Felton R. What's Really in Your Bottled Water?. (2020). <https://www.consumerreports.org/bottled-water/whats-really-in-your-bottled-water/>.
13. Li Y, Fletcher T, Mucs D, et al. Half-lives of PFOS, PFHxS and PFOA after end of exposure to contaminated drinking water. *Occup Environ Med* 75 (2018): 46-51.
14. Olsen GW, Burris JM, Ehresman DJ, et al. Half-life of serum elimination of perfluorooctanesulfonate, perfluorohexanesulfonate, and perfluorooctanoate in retired fluorochemical production workers. *Environ Health Perspect* 115 (2007): 1298-1305.
15. EPA Announces Proposed Decision to Regulate PFOA and PFOS in Drinking Water. (2020). <https://www.epa.gov/newsreleases/epa-announces-proposed-decision-regulate-pfoa-and-pfos-drinking-water>.
16. Working List of PFAS Chemicals with Research Interest and Ongoing Work by EPA. (2020). <https://www.epa.gov/chemical-research/working-list-pfas-chemicals-research-interest-and-ongoing-work-epa>.
17. NIEHS. Perfluoroalkyl and Polyfluoroalkyl Substances (PFAS). (2021). <https://www.niehs.nih.gov/health/topics/agents/pfc/index.cfm>.
18. Erinc A, Melinda BD, Padmanabhan V, et al. Considering environmental exposures to per- and polyfluoroalkyl substances (PFAS) as risk factors for hypertensive disorders of pregnancy. *Environ Res* 197 (2021): 111113.
19. Averina M, Brox J, Huber S, et al. Exposure to perfluoroalkyl substances (PFAS) and dyslipidemia, hypertension and obesity in adolescents. The Fit Futures study. *Environ Res* 195 (2021): 110740.
20. Liao S, Yao W, Cheang L, et al. Association between perfluoroalkyl acids and the prevalence of hypertension among US adults. *Ecotoxicol Environ Saf* 196 (2020): 110589.
21. Min JY, Lee KJ, Park JB, et al. Perfluorooctanoic acid exposure is associated with elevated homocysteine and hypertension in US adults. *Occup Environ Med* 69 (2012): 658-662.
22. Ding N, Gutierrez CK, Mukherjee B, et al. Per- and Polyfluoroalkyl Substances and Incident Hypertension in Multi-Racial/Ethnic Women: The Study of Women's Health Across the Nation. *Hypertension* 79 (2022): 1876-1886.
23. Mi X, Yang YQ, Zeeshan M, et al. Serum levels of per- and polyfluoroalkyl substances alternatives and blood pressure by sex status: Isomers of C8 health project in China. *Chemosphere* 261 (2020): 127691.
24. Bao WW, Qian ZM, Geiger SD, et al. Gender-specific associations between serum isomers of perfluoroalkyl substances and blood pressure among Chinese: Isomers of C8 Health Project in China. *Sci Total Environ* 607 (2017): 1304-1312.
25. Wu Y, Deng M, Jin Y, et al. Toxicokinetics and toxic effects of a Chinese PFOS alternative F-53B in adult zebrafish. *Ecotoxicol Environ Saf* 171 (2019): 460-466.
26. Cui Q, Pan Y, Zhanget H, et al. Occurrence and Tissue Distribution of Novel Perfluoroether Carboxylic and Sulfonic Acids and Legacy Per/Polyfluoroalkyl Substances in Black-Spotted Frog (*Pelophylax nigromaculatus*). *Environ Sci Technol* 52 (2018): 982-990.
27. Luebker DJ, Raymond GY, Kristen JH, et al. Neonatal mortality from in utero exposure to perfluorooctanesulfonate (PFOS) in Sprague-Dawley rats: dose-response, and biochemical and pharmacokinetic parameters. *Toxicology* 215 (2005): 149-169.
28. Dangudubiyam SV, Mishra JS, Zhao H, et al. Perfluorooctane sulfonic acid (PFOS) exposure during pregnancy increases blood pressure and impairs vascular relaxation mechanisms in the adult offspring. *Reprod Toxicol* 98 (2020): 165-173.
29. Dangudubiyam SV, Mishra JS, Song R, et al. Maternal perfluorooctane sulfonic acid exposure during rat pregnancy causes hypersensitivity to angiotensin II and

- attenuation of endothelium-dependent vasodilation in the uterine arteries dagger. *Biol Reprod* 107 (2022): 1072-1083.
30. Furchgott RF, Zawadzki JV. The obligatory role of endothelial cells in the relaxation of arterial smooth muscle by acetylcholine. *Nature* 288 (1980): 373-376.
31. Forsthuber M, Widhalm R, Granitzer S, et al. Perfluorooctane sulfonic acid (PFOS) inhibits vessel formation in a human 3D co-culture angiogenesis model (NCFs/HUVECs). *Environ Pollut* 293 (2022): 118543.
32. Sanghavi M, Rutherford JD. Cardiovascular physiology of pregnancy. *Circulation* 130 (2014): 1003-1008.
33. Qiu Z, Qu K, Luan F, et al. Binding specificities of estrogen receptor with perfluorinated compounds: A cross species comparison. *Environ Int* 134 (2020): 105284.
34. Liu C, Du Y, Zhou B. Evaluation of estrogenic activities and mechanism of action of perfluorinated chemicals determined by vitellogenin induction in primary cultured tilapia hepatocytes. *Aquat Toxicol* 85 (2007): 267-277.